Microfluidic mixing through electrowetting-induced droplet oscillations

F. Mugele, J.-C. Baret, and D. Steinhauser

Microfluidic mixing through electrowetting-induced droplet oscillations

F. Mugele[a)]
Physics of Complex Fluids, University of Twente, P.O. Bus 217, 7500AE Enschede, The Netherlands and Abteilung Angewandte Physik, Universität Ulm, Albert-Einstein-Allee 11, 89069 Ulm, Germany

J.-C. Baret
Physics of Complex Fluids, University of Twente, P.O. Bus 217, 7500AE Enschede, The Netherlands and Philips Research Laboratories Eindhoven, Professor Holstlaan 4, 5656AA Eindhoven, The Netherlands

D. Steinhauser
Abteilung Angewandte Physik, Universität Ulm, Albert-Einstein-Allee 11, 89069 Ulm, Germany

We used electrowetting to trigger self-excited oscillations of millimeter-sized sessile droplets of water-glycerol mixtures in a viscosity range from 1 to 65 mPa s. During the oscillations the contact angle of the droplets varied periodically between $\approx 130°$ and $80°$ with a frequency between 10 and $125\ s^{-1}$, depending on the viscosity and the drop size. By initially staining drops partially with fluorescent dye, we found that the liquid within the drop is completely mixed within 100–2000 oscillation cycles for low and high viscosities, respectively. Compared to pure diffusion, droplet oscillations accelerated mixing by approximately two orders of magnitude for millimeter-sized droplets. © *2006 American Institute of Physics*. [DOI: 10.1063/1.2204831]

Efficient mixing is one of the key challenges in microfluidics.[1,2] Given the small size of microfluidic devices, flow patterns are usually laminar thus preventing turbulent mixing. Low Reynolds number mixing is best achieved by creating chaotic flow patterns within the fluid.[2,3] Earlier mixing studies focused on producing spatially periodic flow profiles in continuous flow systems[4] by patterning the channel walls. More recently droplet-based digital microfluidic systems attracted considerable attention.[5] Mixing within individual droplets has been demonstrated both within continuous flow microchannels[6] and between parallel plates.[7,8] One disadvantage of the existing schemes is that they require a relatively large amount of space on the microfluidic chip because they rely on chaotic internal flow fields generated by translating the droplet. In this letter, we demonstrate that efficient mixing can also be achieved without translating droplets. We show that electrowetting can be used to trigger self-excited droplet oscillations in analogy to previously reported oscillations of capillary bridges.[9] These oscillations are then shown to induce flow fields which speed up mixing within the droplet for a wide range of viscosities.

Droplets of water-glycerol-NaCl mixtures of variable composition ($0-80\%$ vol glycerol, viscosity $\eta = 1-65$ mPa s, [NaCl]$=0.01-0.3$ M, and density $\rho \approx 10^3\ \text{kg/m}^3$) with a volume of $V \approx 1-2\ \mu\text{L}$ were deposited on Si substrates with a 1 μm thick thermally grown SiO_x layer. The latter was covered by a monolayer of octadecyltrichlorosilane following a standard recipe[10] to render the surface hydrophobic at zero voltage. In order to both minimize contact angle hysteresis ($\Delta\theta \approx 2°$ in the present experiments) and prevent evaporation, the experiments were carried out in silicone oil environment (Wacker AK5; viscosity: $\eta_{\text{oil}}=5$ mPa s). Under these conditions, Young's angle was $\theta_Y=155°$. By applying an ac voltage U (frequency $f = 10$ kHz; amplitude $U_{\text{rms}}=0-75$ V) between the substrate

and the droplet via an immersed Pt wire, the contact angle could be reduced to $60°$ following the well-known electrowetting equation[11]

$$\cos\theta(U) = \cos\theta_Y + U^2/U_0^2. \tag{1}$$

Here $U_0=(\varepsilon_0\varepsilon_d)/(2d\sigma_{\text{lo}})$ is the usual electrowetting normalization voltage, ε_0 is the permittivity of vacuum, ε_d and d are the dielectric constant and the thickness of the insulating layer, respectively, and $\sigma_{\text{lo}}=34$ mJ/m^2 is the interfacial tension between the droplet and the ambient oil.

First, we discuss briefly the requirements for achieving self-excited droplet oscillations. Assume that the wire is immersed into the drop at zero voltage at a distance d above the substrate. Upon increasing U, θ decreases and the droplet becomes progressively flatter. At some point a capillary neck forms between the wire and the drop. When U is increased beyond a certain threshold voltage U_T the capillary neck breaks. Provided that the electrical properties of the system are chosen appropriately[12] the drop is completely discharged after breakup. Hence the drop-substrate voltage is zero and θ switches back to $\theta_d \approx \theta_Y$, where θ_d is a dynamic contact angle that is somewhat smaller than θ_Y. (The voltage applied to the wire is left constant at $U=U_T$.) As a result the drop relaxes back towards a spherical cap with $\theta=\theta_Y$ until it touches the wire again. At this moment, θ switches back to $\theta(U)$ and the cycle starts again: the droplet begins to perform self-excited oscillations between the attached and detached morphologies, as shown in Fig. 1. Oscillations were extremely stable and persistent for hours with a well defined frequency f that we measured accurately by monitoring the current in the system. f was found to vary between 20 and 100 Hz, depending on the exact drop size and the viscosity.

Whether droplet oscillations occur or not is determined by the values of the two parameters d and U. Two requirements must be met simultaneously in order to observe oscillations. First, the droplet must detach from the wire during spreading. Second, it must touch the wire again during relaxation. Experimentally, we determined the range of stability of

---
[a)]Author to whom correspondence should be addressed; electronic mail: f.mugele@utwente.nl
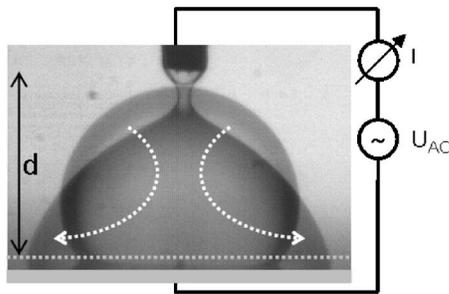
FIG. 1. Overlaid image of droplet shapes for maximum and minimum foot-print areas during oscillations (wire diameter: 250 μm). The dashed and solid horizontal gray lines represent the surface of the insulating layer and the underlying substrate electrode, respectively. The arrows indicate the net displacement of liquid during drop spreading.

the attached and detached morphologies as well as the oscillatory region by varying d and U systematically (Fig. 2). To model the behavior we have to determine the stability limits of both morphologies. If

$$d \lesssim h_0, \tag{2}$$

with h_0 being the drop height at zero voltage, the detached morphology is obviously unstable and hence the second requirement for oscillations is fulfilled. If we express all lengths in units of $V^{1/3}$ this gives rise to a universal horizontal line for fixed θ_Y (solid in Fig. 2). To quantify the first requirement, we need a criterion to determine the capillary breakup, i.e., the stability limit of the attached morphology. As long as the diameter of the wire is small compared to the size of the droplet, we can approximate the attached drop by a spherical cap of contact angle $\theta(U)$ with a small capillary neck of negligible volume on top. Obviously, the capillary neck cannot be stretched to much more than the diameter Φ of the wire. Hence, we adopted the criterion

$$\widetilde{d}_c(U) = d_c(U)/V^{1/3} = \widetilde{h}(\theta) + k\widetilde{\Phi}, \tag{3}$$

with $\widetilde{\Phi} = \Phi/V^{1/3}$ and k being a number of order 1.[13] $\widetilde{h}(\theta) = (\pi/3)^{1/3}(1 - \cos\theta)/(2 - 3\cos\theta + 3\cos^3\theta)^{1/3}$ is the voltage-dependent normalized height of a spherical cap of contact angle θ. The curved solid line in Fig. 2 shows a fit ($k=5$) to the experimental data based on the independently measured electrowetting curve $\theta(U)$. Droplet oscillations occur only when both morphologies are unstable, i.e., in the hatched region which is both above the stability limit of the attached morphology and below the stability limit of the detached morphology. The dotted area corresponds to the region of
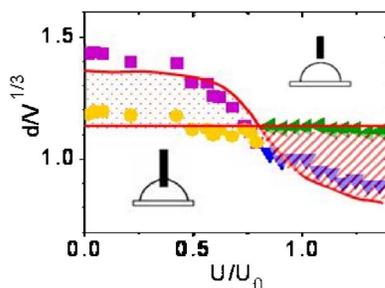

FIG. 2. Morphological diagram. Symbols: experimental stability limits of detached (circles and left triangles) and attached (squares and down triangles) morphologies. Solid lines: model prediction with a best fit value k =5 (see text for details).
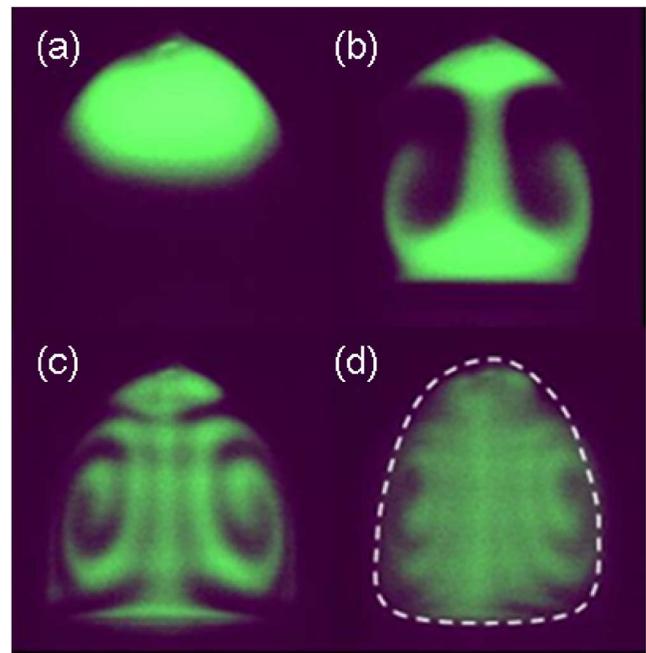

FIG. 3. Dye distribution within oscillating water droplet (oscillation frequency: 81 Hz, lag between images: 45 cycles, i.e., approximately 0.55 s, and drop size $\approx$1 mm). A video sequence is available as additional electronic information.

capillary hysteresis where both morphologies are (meta) stable. In the other regions the drop is either always attached or detached, as indicated in Fig. 2.

In order to follow mixing during the oscillations, we merged two droplets of the same size (one containing fluorescence) such that the top of the resulting larger drop was dye stained whereas the bottom remained dark under epifluorescence observation [Fig. 3(a)]. Once the droplets were merged, the wire was immersed and the voltage was switched on, with d and U previously chosen within the oscillatory region. Side view video snapshots were recorded with a charge coupled device (CCD) camera equipped with a 5$\times$ long working distance microscope objective that was synchronized with the oscillations such that the droplets were always imaged in the same phase of the oscillation cycle. Figure 3 shows the redistribution of the dye within the droplet during the oscillations. The initial dye stained volume is stretched and folded several times giving rise to striation layers of decreasing width, as previously observed in other microfluidic mixing experiments.[4,6] Eventually diffusion blurs the boundaries of the striation layers and gives rise to a homogeneous dye distribution. For pure water, the striation patterns are usually nicely symmetric and the droplets are completely mixed within a few seconds. For higher viscosity the overall scenario is the same; however, the appearance of the dye distribution is less symmetric. Sometimes patches of dye stained liquid move through the droplet and take a long time to redistribute homogeneously. In order to quantify the state of mixing, we calculated the standard deviation σ_I of the fluorescence intensity within the droplet [see dashed line in Fig. 3(d)] and normalized it such that it decreases from a maximum of 1 in the beginning of the experiment to zero in the final completely mixed state. Figure 4 shows a series of typical decay curves for various viscosities. The curves follow the expected decay as the droplet becomes progressively mixed. (The bumps in the higher vis-
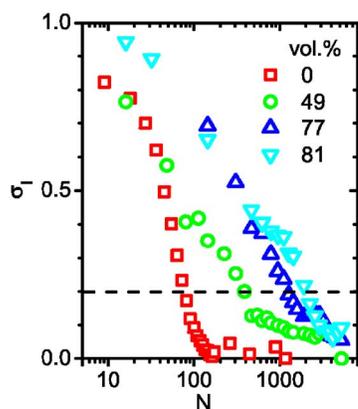
204106-3   Mugele, Baret, and Steinhauser

Appl. Phys. Lett. **88**, 204106 (2006)

FIG. 4. Normalized fluorescence intensity variation vs number of oscillation cycles for various glycerol concentrations. The dashed line ($\sigma_I = 0.2$) defines the threshold level used to indicate mixing.

cosity curves can be traced back to the motion of the just mentioned dye patches.) We adopted the criterion that we denote the droplet as mixed when σ_I has dropped to 20% of its initial value, as indicated by the dashed line in Fig. 4. From the intersection of the data with this line we determine the number of oscillation cycles required to achieve mixing for each viscosity (Fig. 5). Within the present level of accuracy, the number of oscillation cycles appears to increase linearly with the viscosity. From an applied perspective, it is particularly interesting to know by how much mixing is accelerated. Therefore, we used the same criterion as above to determine the diffusive mixing time τ_{diff} monitoring the fluorescence distribution for a nonoscillating droplet over time. In accordance with the expectations $\tau_{\text{diff}} \approx r^2/D$ (r being the droplet radius and D the diffusion constant) was found to range from 5 to 90 min, depending on the viscosity. Hence, mixing is accelerated by more than two orders of magnitude over the entire range of viscosity.

A detailed understanding of mixing during droplet oscillations requires knowledge of the time-dependent flow fields, which is beyond the scope of the present letter.[14] Nevertheless, the evolution of the drop shape indicates some characteristics of the flow: as the drop evolves from the high contact angle state to the low contact angle state in Fig. 1, there is a net displacement of liquid from the central upper part of

the droplet to the lower outer parts, as indicated by the arrows. In an ideal Stokes flow this motion would be perfectly reversed as the drop evolves back to the high contact angle state. Obviously, this is not the case. One origin of symmetry breaking is that the contact angle is low in the spreading and high in the receding phase.[12] Furthermore, high speed movies of oscillating drops show that for low viscosities higher oscillation modes are excited, which contribute further to the asymmetry between the spreading and the receding phase. From the distribution of dye in Fig. 3, we conclude that the downward and outward transport of material during spreading is only partially reversed during the receding motion. As the incomplete reversibility is accumulated over many cycles, the initial dye distribution gets progressively stretched and eventually folded into the observed pattern.

According to standard chaotic advection, the mixing time should increase logarithmically with the Péclet number $\text{Pe} = fr^2/D$,[2,6] which characterizes the relative importance of convective and diffusive transport. This would suggest a logarithmic dependence of the mixing time on the viscosity ($\eta \propto D^{-1}$) instead of the observed linear one in Fig. 5. This deviation is probably related to the fact that changes in the viscosity do not only change Pe but also affect the entire oscillation dynamics and thereby the internal flow patterns. The presence and the absence of higher droplet oscillation modes at low and high viscosities, respectively, are in line with a stronger-than-logarithmic viscosity dependence. More detailed experiments to reveal the flow fields are currently in progress.[15]

The authors thank Bruno Eckhardt for suggesting mixing experiments in combination with droplet oscillations. The authors are also grateful to Stephan Herminghaus for discussions. Financial support by the German Science Foundation within the priority program Wetting and Structure Formation at Interfaces is acknowledged. One of the authors (J.-C.B.) acknowledges support by a Marie Curie Industry Host Contract No. IST-1999-80004.
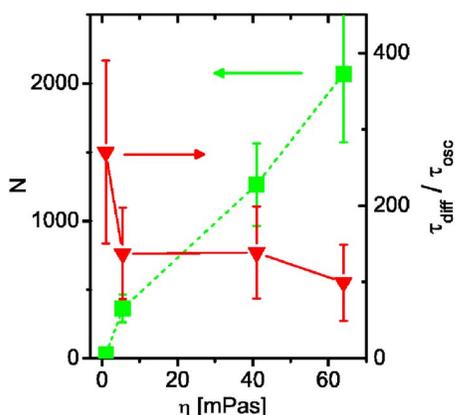

FIG. 5. Number of cycles required for mixing and mixing time ratio for diffusive vs oscillation supported mixing for four different viscosities. Error bars reflect the statistical error over several independent measurements.

[1]T. M. Squires and S. R. Quake, Rev. Mod. Phys. **77**, 977 (2005).
[2]J. M. Ottino and S. Wiggins, Philos. Trans. R. Soc. London, Ser. A **362**, 923 (2004).
[3]H. Aref, Phys. Fluids **14**, 1315 (2002).
[4]A. D. Stroock, S. K. W. Dertinger, A. Ajdari, I. Mezic, H. A. Stone, and G. M. Whitesides, Science **295**, 647 (2002).
[5]See, for instance, special issue of Lab Chip **4**, 292 (2004).
[6]H. Song and R. F. Ismagilov, J. Am. Chem. Soc. **125**, 14613 (2003).
[7]P. Paik, V. K. Pamula, and R. B. Fair, Lab Chip **3**, 253 (2003).
[8]S. K. Cho, H. J. Moon, and C. J. Kim, J. Microelectromech. Syst. **12**, 70 (2003).
[9]A. Klingner, S. Herminghaus, and F. Mugele, Appl. Phys. Lett. **82**, 4187 (2003).
[10]J. Sagiv, J. Am. Chem. Soc. **102**, 92 (1980).
[11]F. Mugele and J.-C. Baret, J. Phys.: Condens. Matter **17**, R705 (2005).
[12]J.-C. Baret and F. Mugele, Phys. Rev. Lett. **96**, 0146106 (2006).
[13]An exact theoretical treatment involving an instability analysis of Delaunay surfaces will be published elsewhere; J.-C. Baret and M. Brinkmann, Phys. Rev. Lett. (submitted).
[14]The flow fields are not known even for the seemingly simple case of spherical cap shaped droplet spreading at constant volume.
[15]See EPAPS Document No. E-APPLAB-88-256620 for a movie file on oscillation-induced mixing in microdroplet. This document can be reached through a direct link in the online article's HTML reference section or via the EPAPS homepage (http://www.aip.org/pubservs/epaps.html).

This article is copyrighted as indicated in the article. Reuse of AIP content is subject to the terms at: http://scitation.aip.org/termsconditions. Downloaded to IP:
129.21.225.52 On: Wed, 18 Jun 2014 14:55:21